VIEWPOINT

Design and Cost Analysis of 100 MW Perovskite Solar Panel Manufacturing Process in Different Locations

Read Online

ACCESS | ▥ Metrics & More | ▤ Article Recommendations | ⓢ Supporting Information

The fast-paced development of perovskite solar cells (PSCs) has rightfully garnered much attention in recent years, exemplified by the improvement in power conversion efficiency (PCE) from 3.8%[1] to over 25%[2,3] in the space of just over a decade. This rapid development provides a window of opportunity for perovskite technology to be commercialized, promising a cheaper alternative to the most widespread types of photovoltaics,[4−6] with lower production costs, material costs, and energy demands during manufacture. Lifecycle assessments of PSCs promise quick energy payback times,[4−6] and some reports suggest low per-watt production costs.[7−10] Furthermore, perovskites may have an opportunity to break through, especially in photovoltaics markets, such as building-integrated, vehicle-integrated, or thin-film flexible PVs, among others, due to the thin active layers and lightweight materials used.

Previous studies comparing perovskite to single-junction (S-J) silicon solar cells predicted a relatively low production cost per panel for PSCs and even a low levelized cost of energy (LCOE) (eq S2).[8,11] Furthermore, all-perovskite tandems offer possible improvements compared with single-junction perovskites, with the best all-perovskite tandems reaching 26.4% efficiency.[12] The tandem devices nevertheless face the same challenges as the S-J PSCs in addition to increased production difficulty. Moreover, the production of silicon used in most solar panels is energy-intensive and worsens the energy payback time (EPBT, eq S3) of both S-J silicon and perovskite-silicon tandem solar panels.[4−6]

We decided to explore the possibility of designing a simple and efficient manufacturing process for PSC panels. Hence, we designed a small-scale, automated pilot line for the manufacture of perovskite solar panels based on slot-dye coating of active layers, conducted partly under a nitrogen atmosphere. This production process was then scaled up and optimized to meet the needs of a moderate-sized commercial production facility. By careful selection of the materials, a configuration of the perovskite active layer viable for commercial-scale manufacture was identified. A bottom-up cost modeling approach was used to determine the material and production costs of the PSCs. Metrics such as minimum sustainable price (MSP, eq S1), LCOE, and EPBT were used to provide an idea of costs associated with the production and use of PSCs manufactured using the proposed process. Finally,

uncertainties related to assumptions used in the calculations are accounted for by sensitivity analysis through a Monte Carlo simulation of the PSC production and installation costs.

■ RESULTS AND DISCUSSION

Material Costs. The material costs can be separated into five main categories: front glass and processing, active layers, back sheet, encapsulation and stringing, and junction box costs (Tables S1 and S2). We have considered multiple options for the active layers of the perovskite cells, i.e., the electron transport layer (ETL) and back-contact material. The five options considered are summarized in Figure 1. The use of different materials impacts not only the direct material costs but also the production process.

Comparing the different back-contact materials, chromium (10 nm) and copper (100 nm) are the cheapest options of those considered. It is assumed that the metals are deposited via thermal evaporation, which takes place under high vacuum conditions. As purging and venting the vacuum chamber requires large amounts of time and energy, the thermal evaporation of metal electrodes is difficult to scale up, and it is uncertain whether it would be commercially viable. The carbon-based back-contact, deposited as a carbon paste, could potentially remove the need of a hole transport layer (HTL).[13−15] Despite this, the layer thickness of the carbon electrode is much higher than that required for metal electrodes (Table S3), mainly due to its lower conductivity, with the thickness reaching up to 60 μm for the most efficient devices.[16] This means a much higher material requirement per m² of panel. Using an optimistic scenario of 2-μm thickness for the carbon layer, options 5 and 6 (Table 1) are the most expensive. The carbon layer thickness should be close to 10 μm to achieve high efficiencies,[17] which would result in $22.7 for the HTL-free option 5 and $23.5 per m² with the addition of an HTL. Another option is a metal ink or paste. Given that silver ink can produce a well-formed electrode layer, it presents
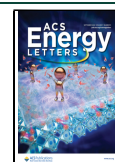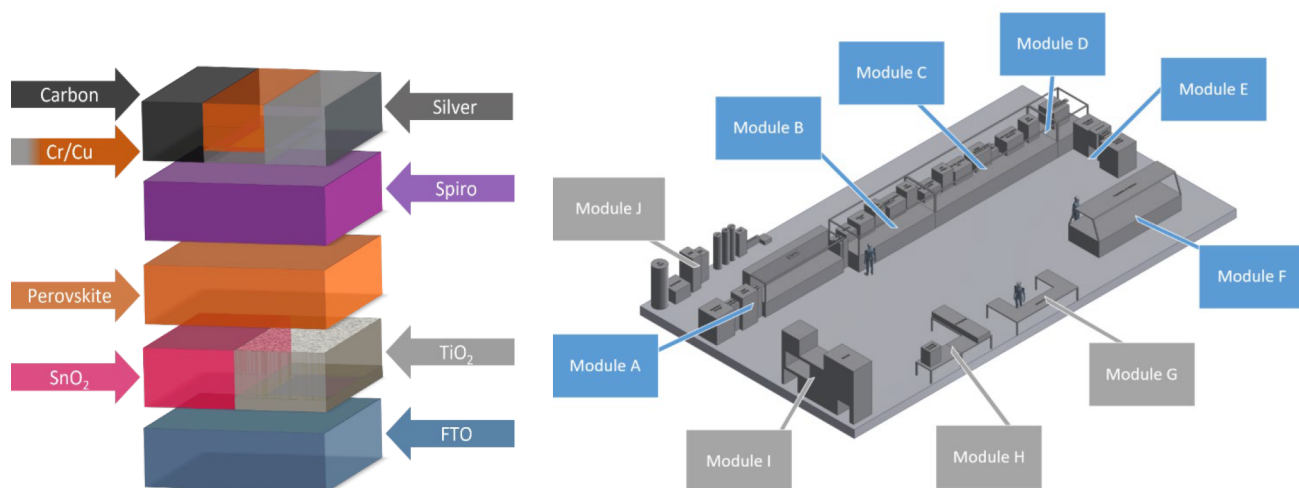
Figure 1. (Left) Visual representation of the active layer material configurations considered in this study. (Right) 3D model of pilot line production of perovskite solar cells this study uses as a basis for a scale-up to a 100 MW annual production. Module A: Loading, laser scribing and cleaning. Module B: Etching, spray coating, slot die coating and annealing. Module C: Slot die coating, annealing and laser scribing. Module D: Encapsulation, Module E: Unloading, testing and stocking. Module F: Solution preparation. Module G: Monitoring/ quality control desk. Module H: Prototyping area. Module I: Storage. Module J: Auxiliary equipment, compressor, gas and nitrogen tank, and water treatment.

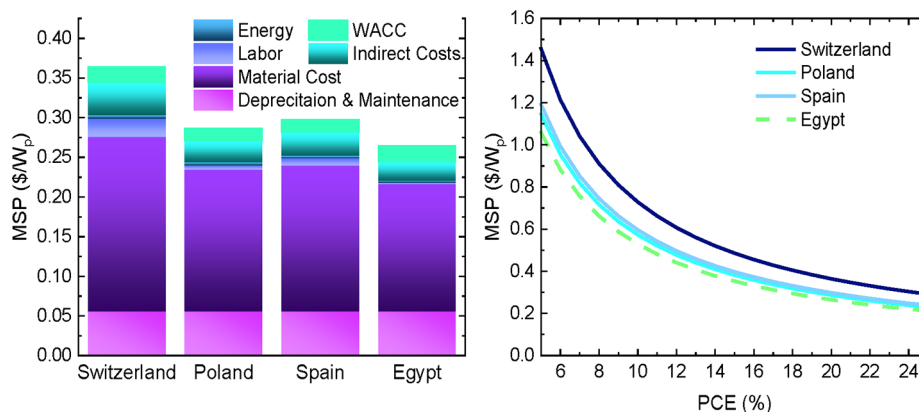| Layer	Option 1	Option 2	Option 3	Option 4	Option 5
ETL 1	c-TiO$_2$	c-TiO$_2$	SnO$_2$	SnO$_2$	c-TiO$_2$
ETL 2	m-TiO$_2$	m-TiO$_2$			m-TiO$_2$
Perovskite	Perovskite	Perovskite	Perovskite	Perovskite	Perovskite
HTM	Spiro	Spiro	Spiro	Spiro	-
Electrode	Cr/Cu	Silver Ink	Cr/Cu	Silver Ink	C-Paste
Price/m2 (100 MW)	$5.9	$6.6	$2.7	$3.4	$8.1
Price/m2 (1 GW)	$5.0	$5.1	$1.9	$2.0	$6.2

Figure 2. (Table) Summary of the active layer configurations. Options 1, 2, and 5 using compact and meso TiO$_2$ deposited through spray pyrolysis and slot-die coating. Options 3 and 4 using slot-die coated colloidal solution of SnO$_2$. (Graphs) Options 1 and 3 consider chromium and copper deposited in two steps through thermal evaporation. The other electrodes are silver ink and carbon paste deposited through a slot-die process. A column graph showing the individual elements of MSP at 20% PCE (Left) in Egypt, Spain, Poland, and Switzerland and curves representing the relationship between MSP and PCE (Right).

the best compromise between easy deposition and low material cost. The electrode can be deposited via slot-die coating followed by annealing. This material was therefore used for calculations in the rest of the cost analysis unless stated otherwise.

Two candidate ETLs were identified. The first uses compact and mesoporous TiO$_2$ layers and would require two coating and annealing steps at a temperature level of approximately 450 °C. The mesoporous layer is expensive relative to the

other layers, comprising close to 51% of the overall active layer costs in option 2. The second ETL candidate is a single tin oxide layer deposited either from a SnCl$_2$ solution or an SnO$_2$ colloidal dispersion. These solutions are deposited either through spray pyrolysis[18] or slot dye coating already used in commercial production.[19−21] In options 3 and 4 (see the Table in Figure 2), it is assumed that the tin oxide layer is made through slot-die deposition of a colloidal SnO$_2$ solution in water as described by Bu et al.[21] Option 4 with an SnO$_2$ ETL
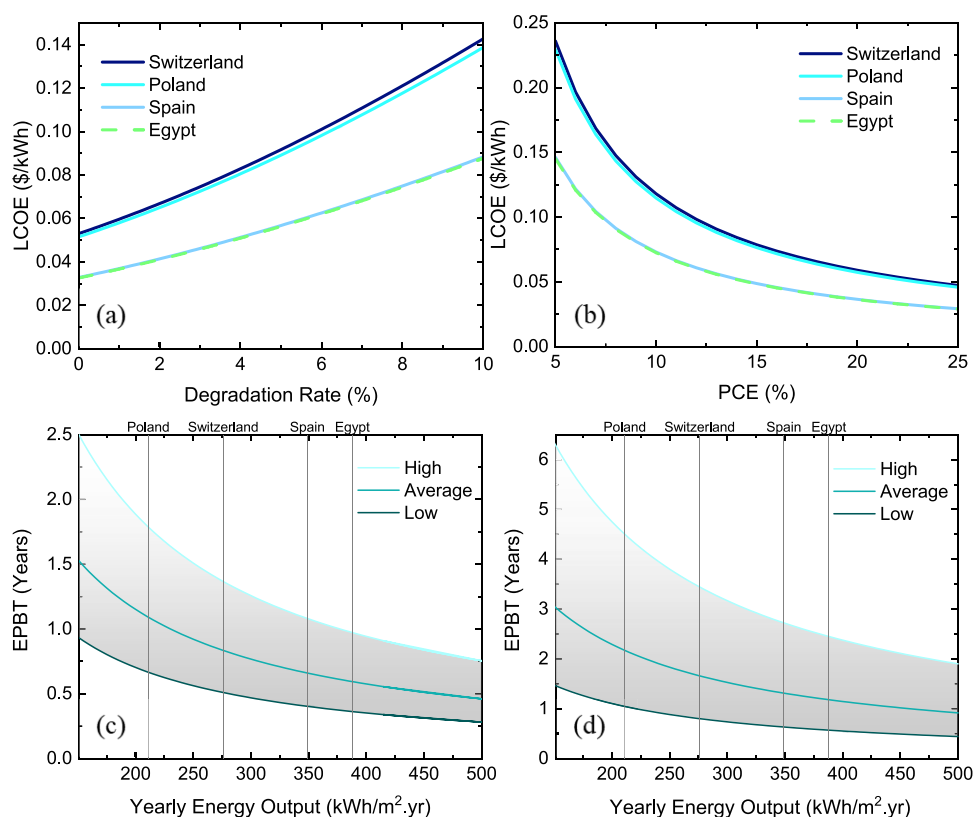
Figure 3. (a) LCOE dependence on degradation rate and (b) PCE based on production and installation costs in Switzerland, Poland, Spain, and Egypt. (c) EPBT of perovskite solar panels without installation and (d) with installation. High and low curves represent the pessimistic and optimistic scenarios, respectively. The average curve is a geometric average of the two values.

and Ag electrode has fewer deposition steps, fewer energy requirements for annealing, and lower material costs.

Both tin oxide and c-TiO$_2$/m-TiO$_2$ are common ETL choices, and high efficiencies can be achieved using either (Table S4).[2,3,22−26] Furthermore, in all the reported investigations, Spiro-OMeTAD HTL is used along with an Au electrode. The limitation of gold electrodes is their prohibitively high cost.[27] Silver was identified as one of the more economical replacements. A study comparing the efficiencies of different electrodes found only a 0.15% PCE reduction when using Ag as opposed to Au.[28] This shows that Ag does not significantly harm the device performance. The more prominent issue with Ag-based electrodes is their tendency to degrade when exposed to the iodine ions present in the perovskite and thus reduced lifetime. Methods have been proposed to counter this issue by suppressing ion migration with good results,[29] and it is possible the Ag cells might recover some of the lost performance through aging, therefore not requiring additional corrosion protection.[30]

Energy Consumption and Production Process. The production process should be primarily based on slot-die coating of the active layers onto an FTO glass substrate. The process is displayed in Figure 1 which shows all basic steps. The input parameters for the pilot and 100 MW plans can be found in the SI (Table S5).

Comparing the different options from the previous section, using different materials would also result in changes in the production process and inevitably to the production costs. This would impact the operating and capital expenditure of production. Fewer process steps mean less equipment necessary in the process, thereby reducing cost. In this regard,

options 3 and 4 (Table in Figure 2) are better than the others. Energy use would also decrease, most notably in option 4, where fewer sintering steps are needed, resulting in significant reductions in energy consumption. Option 4 would also result in lower material cost compared to option 2. From an operational perspective, option 4 is the least expensive and requires the fewest production steps.

The energy consumption of each production step has been factored. The c-TiO$_2$ and m-TiO$_2$ deposition steps are the most energy demanding (Figure S1). This is a consequence of the two energy-demanding sintering steps at a temperature of 450 °C. Compared with the SnO$_2$ deposition, where the single sintering requires only 150 °C, the ETL deposition in options 2 and 5 consumes more than 6 times the energy (Table S6). The energy consumption of the sintering steps, however, depends on the efficiency of the process and could be reduced with the use of more efficient equipment.

The MSP per Watt peak (Wp) reported in previous studies ranges from 0.25 to 0.69 $/Wp for perovskite solar panels.[7−10,31−33] The MSP of silicon panels ranges from 0.34 $/Wp for panels manufactured in China to 0.54 $/Wp for panels manufactured in Germany according to an NREL report.[34] A further report suggests an MSP of 0.25−0.27 $/Wp for silicon panels and an MSP of 0.38 $/Wp for perovskite solar panels manufactured at small scale with possible reductions to 0.18 $/Wp for larger scale.[35] The differences in MSP predicted for the perovskite solar panels are due to the starting conditions and assumptions used. Different materials and manufacturing processes were evaluated with some studies assuming a plant capacity of 100−200 MW.[9,31−34] Notably, the scale of the production has a significant impact on the

production costs as economies of scale dictate. This was also shown by Mathews et al. for a production capacity of up to 1 GW.[32] In Table S7, a summary of assumptions used is provided, which includes, importantly, labor costs, overhead costs, and the weighted average cost of capital (WACC).

The summary of the MSPs in Figure 2 reveals a difference between all four countries considered in this study. The MSP in Switzerland is the highest ($73/m^2), due to higher material costs. This is primarily a consequence of the high labor cost of glass processing in Switzerland, which are markedly higher than those in other countries. The MSP in the other countries ranges from $53−60 per m^2 with the prices being lowest in Egypt. The graphs also show a relatively low variability of MSP between Egypt, Poland, and Spain, where the MSP stays within 10% error of 28.5 ¢/Wp. The MSP in Switzerland is 26% higher than the MSP in Poland, which is still within a reasonable margin. The main difference between the MSP in Switzerland and other countries is not the labor during final production but rather the glass processing prices. If this difference could be overcome, then results would be much more favorable for the Swiss manufacture.

Levelized Cost of Energy. The variation of the MSP is largely dependent on the local economy; however, the LCOE depends also on the capability of the perovskite solar panels to generate electricity (Table S9). This is mostly defined by the solar illumination at the location of the solar farm installation, as well as the loss factor. Additionally, the perovskite PV installation is assumed to be a commercial ground-mount installation. The scale of the installation would also impact the associated installation costs, which are examined more closely in the sensitivity analysis section.

The LCOE values were calculated at 3.6, 3.6, 5.7, and 5.9 ¢/kWh in Egypt, Spain, Poland and Switzerland, respectively. In comparison, the currently used PV technologies, notably c-Si and GIGS, achieve LCOE values between 7 and 13 ¢/kWh across the United States according to a study from 2015[36] and Si crystalline PV have LCOE values of 7−10 ¢/kWh for ground-mount commercial systems,[37] which is comparable to the scale of production discussed in this study. The silicon PV LCOE can reach 4−6 ¢/kWh for utility-scale applications in the United States,[37] which is slightly higher than our results ranging from 3.6 to 5.9 ¢/kWh. This means a similar LCOE can be achieved by perovskite solar panels manufactured at relatively small scales, with reduced starting capital investment requirements. This could be of crucial importance in determining the pace at which the perovskite technology enters the commercial sphere.

Figure 3 shows the relationship between LCOE and the yearly degradation rate, which demonstrates the need to maintain a low degradation rate to minimize the LCOE. However, considering a shift of the degradation rate from 0.9% to 2% per year, the LCOE would increase by 13% at all of the geographic locations considered. Even doubling of the panel degradation rate results in only a moderate change in the LCOE. A degradation rate of 2% would still result in LCOEs ranging from 4 to 6.7 ¢/kWh, thus keeping the perovskite technology competitive. Nevertheless, improving perovskite stability remains a key factor in achieving a low LCOE.

Another factor to be considered concerning the LCOE is the perovskite solar panel PCE (Figure 3). Increasing the PCE is one of the main targets of current perovskite research, with the single-junction perovskite theoretical limit surpassing 30% efficiency.[38] An encouraging result at 13% efficiency was obtained, with the perovskite LCOE still falling below 10 ¢/kWh. To get below the LCOE of Si-based panels, the PCE would ideally need to be above 18%, since this would keep the perovskite LCOE in all four countries below the 7−10 ¢/kWh range of commercial silicon applications as discussed above.[37]

Energy Payback Time. In prior work, the EPBT was reported to be significantly lower for thin-film photovoltaics than perovskite solar panels.[4−6] Our results point to a range of possible EPBT values, based on different embedded energy estimates taken from the literature.[39−44] The resulting calculated EPBTs range from 2.2 years in Poland to 1.2 years in Spain for ground-mount perovskite systems. The EPBTs ranges from 1.1 to 0.6 years for a perovskite solar panel without installation costs (Table S10). The perovskite panel production process only accounts for 5.7% of the overall energy input of an installed panel and 11.3% of a panel without installation. The rest of the input energy is associated with transportation, energy overhead, and material embedded energy where the perovskite active layers make up less than 1% of the installed panel input energy.

The EPBT lower and upper bounds of the installed and noninstalled panels are summarized in Figure 3. The EPBT is strongly influenced by the energy output of the perovskite PV system and the error bounds around the geometric average are significant. This shows that no single parameter can easily describe the EPBT for the perovskite technology. Nevertheless, it can also be seen that the embedded energy of the perovskite active layers, together with the production process, constitute only a small fraction (6.5%) of the installed panel input energy and the production process has relatively low energy requirements, especially when compared with conventional silicon-based photovoltaics.[4−6]

Sensitivity Analysis and Monte Carlo Simulations. A sensitivity analysis has helped to establish the lower and upper bounds of the MSPs and installation costs. The standard distributions of the MSPs generated by the simulation can be found in the SI (Figure S2). Mean, lower, and upper estimate values were obtained from these standard distributions. The main results of the Monte Carlo simulations are presented in Figure S3. Looking at the different regions, in terms of MSP and LCOE it is possible to observe key variations. The effect of the local labor and material costs is marginal, with the OECD countries of Poland and Spain ranging from 27 to 33 ¢/Wp and Egypt from 24 to 29 ¢/Wp.

The effects of the manufacturing cost are less visible in the LCOE, and the local illumination and maintenance/installation costs seem to be the more important factors. The best-case LCOE in Egypt is 3.1 ¢/kWh, and the worst-case LCOE in Switzerland is 6.8 ¢/kWh. A LCOE of 6.8 ¢/kWh is still below the previously mentioned LCOE of commercial c-Si PVs.[37]

The sensitivity analysis has revealed the importance of reducing the cost of multiple key parameters, such as material costs, equipment cost and installation. The largest and most variable components of the material costs are the front glass and encapsulation (Table S11). A reduction of glass processing prices and use of cheap encapsulation materials could reduce final costs considerably. Furthermore, focusing on creating a simple and efficient production process with as few steps as possible would further reduce the final price. Lastly, the installation cost is made up of many smaller components. Two areas to reduce costs could be to build on less expensive (or multiuse) land and reducing the labor needed for installation.

CONCLUSIONS

A cost analysis based on the bottom-up modeling approach and scale-up of a pilot line design for the production of perovskite solar panels has been performed. This analysis allows the material costs and equipment costs associated with perovskite PV production to be estimated. Furthermore, we have compared the impact of selecting different ETL and counter-electrode materials on the material cost, production process, and energy requirements. The use of a SnO_2 ETL and a metal paste (Ag) results in fewer processing steps, comparable or lower material costs, and lower energy consumption compared with other alternatives presented in this study. Multiple locations were selected for the calculation of MSP, LCOE, and EPBT. Significant variance was found in all metrics between the selected locations, which was considerably affected by local glass processing prices. The LCOE was significantly impacted by the yearly solar illumination at the selected locations, and wages and land prices associated with panel installation. The EPBT was calculated to be as low as 0.6 years for standalone perovskite solar panels in Egypt and 1.1 years for ground-mount perovskite panels. However, in Poland, the EPBT times were as high as 1.1 years for standalone and 2.2 years for installed perovskite panels. Furthermore, there is a great disparity in embedded energy values presented in the literature, which could lead to large errors in EPBT calculations. Nevertheless, it was established that the production process itself is not very energy demanding and requires only 5.6 kWh/m^2 in the best case. The Monte Carlo simulation predicted that the LCOE can range between 3 and 4 ¢/kWh in more sunny locations, such as Spain or Egypt. Overall, perovskite PV production has the potential of being competitive with other PV technologies even at smaller scales of production, assuming the stability of the solar cells is sufficient, and the lab-made perovskite efficiency translates well into larger perovskite modules.

Pavel Culík

Keith Brooks

Cristina Momblona ⊙ orcid.org/0000-0003-2953-3065

Martin Adams

Sachin Kinge

François Maréchal

Paul J. Dyson ⊙ orcid.org/0000-0003-3117-3249

Mohammad Khaja Nazeeruddin ⊙ orcid.org/0000-0001-5955-4786

ASSOCIATED CONTENT

ⓈⅠ Supporting Information

The Supporting Information is available free of charge at https://pubs.acs.org/doi/10.1021/acsenergylett.2c01728.

Full description of the methods, bottom-up modeling, minimum sustainable price, levelized cost of energy, energy payback time, solar panel assumptions, materials' costs, perovskite manufacturing plant costs, and Monte Carlo simulations (PDF)

AUTHOR INFORMATION

Complete contact information is available at:
https://pubs.acs.org/10.1021/acsenergylett.2c01728

Notes

The authors declare no competing financial interest.

ACKNOWLEDGMENTS

REFERENCES

(1) Kojima, A.; Teshima, K.; Shirai, Y.; Miyasaka, T. Organometal halide perovskites as visible-light sensitizers for photovoltaic cells. *J. Am. Chem. Soc.* **2009**, *131*, 6050.

(2) Yoo, J. J.; et al. Efficient perovskite solar cells via improved carrier management. *Nature* **2021**, *590*, 587.

(3) Min, H.; et al. Perovskite solar cells with atomically coherent interlayers on SnO2 electrodes. *Nature* **2021**, *598*, 444.

(4) Tian, X.; Stranks, S. D.; You, F. Life cycle energy use and environmental implications of high-performance perovskite tandem solar cells. *Sci. Adv.* **2020**, *6*, eabb0055.

(5) Celik, I.; et al. Life Cycle Assessment (LCA) of perovskite PV cells projected from lab to fab. *Sol. Energy Mater. Sol. Cells* **2016**, *156*, 157.

(6) Leccisi, E.; Fthenakis, V. Life cycle energy demand and carbon emissions of scalable single-junction and tandem perovskite PV. *Prog. Photovoltaics Res. Appl.* **2021**, *29*, 1078.

(7) Cai, M.; Wu, Y.; Chen, H.; Yang, X.; Qiang, Y.; Han, L. Cost-Performance Analysis of Perovskite Solar Modules. *Adv. Sci.* **2017**, *4*, 1600269.

(8) Song, Z.; et al. Manufacturing Cost Analysis of Perovskite Solar Modules in Single-Junction and All-Perovskite Tandem Configurations. *2018 IEEE 7th World Conference on Photovoltaic Energy Conversion, WCPEC 2018 - A Joint Conference of 45th IEEE PVSC, 28th PVSEC and 34th EU PVSEC* **2018**, 1134−1138.

(9) Kajal, P.; Verma, B.; Vadaga, S. G. R.; Powar, S. Costing Analysis of Scalable Carbon-Based Perovskite Modules Using Bottom Up Technique. *Glob. Challenges* **2021**, *6*, 2100070.

(10) Sofia, S. E.; et al. Roadmap for cost-effective, commercially-viable perovskite silicon tandems for the current and future PV market. *Sustain. Energy Fuels* **2020**, *4*, 852.

(11) Zafoschnig, L. A.; Nold, S.; Goldschmidt, J. C. The Race for Lowest Costs of Electricity Production: Techno-Economic Analysis of Silicon, Perovskite and Tandem Solar Cells. *IEEE J. Photovoltaics 10* **2020**, *10*, 1632.

(12) Lin, R.; et al. All-perovskite tandem solar cells with improved grain surface passivation. *Nature* **2022**, *603*, 73.

(13) Kartikay, P.; Yella, A.; Mallick, S. Hole transport layer free stable perovskite solar cell with low temperature processed carbon electrodes. *Conference Record of the IEEE Photovoltaic Specialists Conference* **2019**, 0473−0476.

(14) Zheng, X. Boron Doping of Multiwalled Carbon Nanotubes Significantly Enhances Hole Extraction in Carbon-Based Perovskite Solar Cells. *Nano Lett.* **2017**, *17*, 2496.

(15) Yue, G.; Chen, D.; Wang, P.; Zhang, J.; Hu, Z.; Zhu, Y. Low-temperature prepared carbon electrodes for hole-conductor-free mesoscopic perovskite solar cells. *Electrochim Acta* **2016**, *218*, 84−90.

(16) Zhang, H.; et al. High-efficiency (>20%) planar carbon-based perovskite solar cells through device configuration engineering. *J. Colloid Interface Sci.* **2022**, *608*, 3151.

(17) Zhang, F.; et al. Engineering of hole-selective contact for low temperature-processed carbon counter electrode-based perovskite solar cells. *J. Mater. Chem. A* **2015**, *3*, 24272.

(18) Taheri, B.; Calabro, E.; Matteocci, F.; Di Girolamo, D.; Cardone, G.; Liscio, A.; Di Carlo, A.; Brunetti, F. Automated Scalable Spray Coating of SnO2 for the Fabrication of Low-Temperature Perovskite Solar Cells and Modules. *Energy Technol.* **2020**, *8*, 1901284.

(19) Chapagain, S.; et al. Direct Deposition of Nonaqueous SnO2Dispersion by Blade Coating on Perovskites for the Scalable Fabrication of p-i-n Perovskite Solar Cells. *ACS Appl. Energy Mater.* **2021**, *4*, 10477.

(20) He, R.; Nie, S.; Huang, X.; Wu, Y.; Chen, R.; Yin, J.; Wu, B.; Li, J.; Zheng, N. Scalable Preparation of High-Performance ZnO−SnO2 Cascaded Electron Transport Layer for Efficient Perovskite Solar Modules. *Sol. RRL* **2021**, *5*, 2100188.

(21) Bu, T.; et al. Universal passivation strategy to slot-die printed SnO 2 for hysteresis-free efficient flexible perovskite solar module. *Nat. Commun.* **2018**, *9*, 4609.

(22) Jeong, J.; et al. Pseudo-halide anion engineering for *α*-FAPbI3 perovskite solar cells. *Nature* **2021**, *592*, 381.

(23) Zhang, J.; Li, R.; Apergi, S.; Wang, P.; Shi, B.; Jiang, J.; Ren, N.; Han, W.; Huang, Q.; Brocks, G.; Zhao, Y.; Tao, S.; Zhang, X. Multifunctional Molecule Engineered SnO2 for Perovskite Solar Cells with High Efficiency and Reduced Lead Leakage. *Sol. RRL* **2021**, *5*, 2100464.

(24) Jeong, M.; et al. Stable perovskite solar cells with efficiency exceeding 24.8% and 0.3-V voltage loss. *Science* **2020**, *369*, 1615.

(25) Jang, Y. W.; et al. Intact 2D/3D halide junction perovskite solar cells via solid-phase in-plane growth. *Nat. Energy* **2021**, *6*, 63.

(26) Kim, G.; et al. Impact of strain relaxation on performance of α-formamidinium lead iodide perovskite solar cells. *Science* **2020**, *370*, 108.

(27) Bloomberg. XAU:CUR. Bloomberg.com. See the following: https://www.bloomberg.com/quote/XAU:CUR (accessed February 10, 2022).

(28) Xiao, J.-W.; Shi, C.; Zhou, C.; Zhang, D.; Li, Y.; Chen, Q. Contact Engineering: Electrode Materials for Highly Efficient and Stable Perovskite Solar Cells. *Solar RRL* **2017**, *1*, 1700082.

(29) Lin, C.-T.; Ngiam, J.; Xu, B.; Chang, Y.-H.; Du, T.; Macdonald, T. J.; Durrant, J. R.; McLachlan, M. A. Enhancing the operational stability of unencapsulated perovskite solar cells through Cu−Ag bilayer electrode incorporation. *J. Mater. Chem. A* **2020**, *8*, 8684−8691.

(30) Lee, D. G.; et al. Effect of Metal Electrodes on Aging-Induced Performance Recovery in Perovskite Solar Cells. *ACS Appl. Mater. Interfaces* **2019**, *11*, 48497.

(31) Chang, N. L.; et al. A manufacturing cost estimation method with uncertainty analysis and its application to perovskite on glass photovoltaic modules. *Prog. Photovoltaics Res. Appl.* **2017**, *25*, 390.

(32) Mathews, I.; et al. Economically Sustainable Growth of Perovskite Photovoltaics Manufacturing. *Joule* **2020**, *4*, 822.

(33) Song, Z.; et al. A technoeconomic analysis of perovskite solar module manufacturing with low-cost materials and techniques. *Energy Environ. Sci.* **2017**, *10*, 1297.

(34) Woodhouse, M.; Smith, B.; Ramdas, A.; Robert, M. *Crystalline Silicon Photovoltaic Module Manufacturing Costs and Sustainable Pricing: 1H 2018 Benchmark and Cost Reduction Roadmap*; National Renewable Energy Laboratory, 2019. See the following: https://www.nrel.gov/docs/fy19osti/72134.pdf.

(35) Smith, B. L. et al. *Photovoltaic (PV) Module Technologies: 2020 Benchmark Costs and Technology Evolution Framework Results*; National Renewable Energy Laboratory and Independent Contractor, 2021 See the following: https://www.nrel.gov/docs/fy22osti/78173.pdf.

(36) Jones-Albertus, R.; Feldman, D.; Fu, R.; Horowitz, K.; Woodhouse, M. Technology advances needed for photovoltaics to achieve widespread grid price parity. *Prog. Photovoltaics Res. Appl.* **2016**, *24*, 1272.

(37) Feldman, D. et al. *U.S. Solar Photovoltaic System and Energy Storage Cost Benchmark: Q1 2020*; National Renewable Energy Laboratory, 2021. See the following: https://www.nrel.gov/docs/fy21osti/77324.pdf.

(38) Wu, T.; et al. The Main Progress of Perovskite Solar Cells in 2020−2021. *Nano-Micro Letters* **2021**, *13*, 152.

(39) Mann, S. A.; De Wild-Scholten, M. J.; Fthenakis, V. M.; Van Sark, W. G. J. H. M.; Sinke, W. C. The energy payback time of advanced crystalline silicon PV modules in 2020: A prospective study. *Progress in Photovoltaics: Research and Applications* **2014**, *22*, 1180.

(40) Peng, J.; Lu, L.; Yang, H. Review on life cycle assessment of energy payback and greenhouse gas emission of solar photovoltaic systems. *Renewable and Sustainable Energy Reviews* **2013**, *19*, 255.

(41) Gong, J.; Darling, S. B.; You, F. Perovskite photovoltaics: Life-cycle assessment of energy and environmental impacts. *Energy Environ. Sci.* **2015**, *8*, 1953.

(42) Correa Guerrero, N. B.; Herrera Martínez, W. O.; Civit, B.; Perez, M. D. Energy performance of perovskite solar cell fabrication in Argentina. A life cycle assessment approach. *Sol. Energy* **2021**, *230*, 645−653.

(43) Nawaz, I.; Tiwari, G. N. Embodied energy analysis of photovoltaic (PV) system based on macro- and micro-level. *Energy Policy* **2006**, *34*, 3144.

(44) Jungbluth, N.; Stucki, M.; Photovoltaics, F. R. *Sachbilanzen von Energiesystemen: Grundlagen für den ökologischen Vergleich von Energiesystemen und den Einbezug von Energiesystemen in Ökobilanzen für die Schweiz*; ecoinvent report No. 6-XII. Swiss Cent. Life Cycle Invent. Dübendorf, CH 16-69; Bundesamt für Energiewirtschaft (BEW) Projekt- und Studienfonds der Elektrizitätswirtschaft (PSEL), 2009. See the following: https://www.psi.ch/sites/default/files/import/ta/PublicationTab/Frischknecht_1996.pdf.